Journal of Catalysis **183,** 384–395 (1999)
Article ID jcat.1999.2400, available online at http://www.idealibrary.com on IDEAL®

Influence of the Hydrogenation Step on Selectivity during the Nonoxidative Oligomerization of Methane to Alkanes on Pt/SiO_2 Catalysts (EUROPt-1)

Eric Marceau,*,[1] Jean-Michel Tatibouët,*,[2] Michel Che,*,[3] and Jacques Saint-Just†

*Laboratoire de Réactivité de Surface, UMR CNRS 7609, Université Pierre et Marie Curie (Paris VI), 4 place Jussieu, 75252 Paris Cedex 05, France; and †Gaz de France—Direction de la Recherche, 361 avenue du Président Wilson—BP 33, 93211 Saint-Denis La Plaine Cedex, France

Received September 25, 1998; revised December 18, 1998; accepted December 21, 1998

Methane oligomerization to alkanes can be accomplished on supported platinum via a two-step procedure: formation of carbonaceous species on the metallic surface by methane adsorption, followed by hydrogenation of these species. Temperature-programmed oxidation (TPO) experiments performed after hydrogenation steps of various durations show that the hydrogenation of a carbonaceous deposit obtained at 300°C on the reference Pt/SiO_2 catalyst EUROPt-1 is not a fast process. Two groups of surface carbonaceous species have been characterized through their different reactivities toward oxygen, but at 300°C their reactivities toward hydrogen are similar. Among alkanes up to C_5, methane is the main product of hydrogenation, corresponding to one-half of the surface carbon reactive toward hydrogen; linear and branched alkanes are produced from the other half of the reactive carbonaceous species. On EUROPt-1, mainly ethane and *n*-pentane are produced during the first minutes of reaction, while on a sintered catalyst the initial production in *n*-pentane is negligible. The release of *n*-pentane during an intermediate purge with inert gas on EUROPt-1 shows that C–C bonds can form already during methane adsorption, leading to C_5 precursors on specific active sites of this catalyst maybe coordinately unsaturated platinum atoms. A model of formation of C_5 precursors is proposed by analogy with the organometallic chemistry of molecular hydrocarbon platinacycles. The subsequent production of alkanes ($C_2 > C_3 > C_4 > C_5$) could be described through a statistical model of dynamic coupling between carbonaceous species involving hydrogen, rather than by hydrogenolysis of heavier carbonaceous species. However, this latter mechanism is likely to predominate for the production of C_6–C_8 compounds.

Key Words: **methane oligomerization; platinum; EUROPt-1; hydrogenation.**

INTRODUCTION

Methane is the main component of natural gas, presently the second source of fossil energy behind oil. It is considered to be a "clean" fuel, thanks to a high H/C ratio, which allows natural gas to provide more energy per mole of CO_2 released than coal or oil (1). However, two obstacles limit its further valorization: (i) natural gas exists in large quantities, but in remote areas, with associated high transportation costs; (ii) the nature of the CH_4 molecule (strong equivalent C–H bonds, absence of polarity, no functional groups) makes its chemical conversion to transportable liquid hydrocarbons energy intensive (1–4). Heterogeneous catalytic processes leading to hydrocarbons from methane have been investigated and most of them are representative of the indirect routes (2): Fischer–Tropsch synthesis carried out on metallic supported catalysts requires the prior catalytic reforming of methane to "synthesis gas," i.e., the mixture CO/H_2 (5); the Mobil process consists of the homologation of methanol on acidic solids (ZSM-5 zeolite), which requires the intermediate synthesis of methanol from CO/H_2 (6). An alternative route is direct methane conversion. This search has given interesting results, under oxidative conditions (oxidative coupling of methane to ethane and ethylene, OCM) as well as, more fundamentally at the present time, under nonoxidative conditions (aromatization in argon beam, synthesis of aromatics on zeolites and superacids, formation of hydrocarbons in membrane reactors, etc.) (7, 8). Among these reactions, methane nonoxidative oligomerization to alkanes on supported metals is one of the most recently investigated (8, 9). Light hydrocarbons can actually be obtained by hydrogenation of carbonaceous species that were previously deposited on a metallic surface (Co, Ru, Rh, Pd, Ir, Pt) via methane adsorption in flow conditions. This two-step sequence involves a solid reactant used to circumvent the unfavorable thermodynamics of the following family of reactions:

$$n\mathrm{CH_4} \rightarrow \mathrm{C}_n\mathrm{H}_{2n+2} + (n-1)\mathrm{H_2}, \quad \Delta G > 0.$$

[1] To whom correspondence should be addressed. Fax: 33 1 44 27 60 33. E-mail: marceau@ccr.jussieu.fr.

[2] Current address: Laboratoire de Catalyse en Chimie Organique, UMR CNRS 6503, ESIP, Université de Poitiers, 40 avenue du recteur Pineau, 86022 Poitiers Cedex, France.

[3] Institut Universitaire de France.

0021-9517/99 $30.00

The same principle also applies to the coupling between methane and olefins (10) or between olefins (11) to yield higher hydrocarbons.

To achieve the production of hydrocarbons, the operating conditions of the first step (methane adsorption on the catalyst surface),

$$CH_{4(g)} + \text{catalyst} \leftrightarrows \text{carbonaceous species}_{ads} + H_{2(g)},$$

and of the second step (hydrogenation of carbonaceous species formed during the first step),

$$\text{carbonaceous species}_{ads} + H_{2(g)} \leftrightarrows C_nH_{2n+2(g)} + \text{catalyst},$$

must be optimized and two procedures based on different hypotheses were independently proposed 7 years ago:

1. Van Santen and co-workers used a dual-temperature sequence to favor thermodynamics in each step (fast methane adsorption at ≈400°C, then cooling and hydrogenation at ≈100°C), supposing that the aging of carbon deposits at high temperature could lead to species alike to metallic carbides, unreactive toward hydrogen (12, 13). C–C bonds were supposed to be created during the hydrogenation step, which could be theoretically confirmed for cobalt and ruthenium, but could not be proved for a temperature of 100°C on platinum, known to be a poor catalyst for similar Fischer–Tropsch reactions (14). Moreover, the slate of hydrocarbons produced on platinum in the second step of the procedure could not verify the Anderson–Schulz–Flory statistical distribution associated with the Fischer–Tropsch synthesis (15).

2. In contrast, Amariglio *et al.* performed most of their experiments under isothermal conditions (both steps performed at the same temperature, 200–320°C). The thermodynamical limitation was explained to be circumvented additionally by the different hydrogen partial pressures existing between the first step (elimination via the gas flow) and the second step (hydrogenation) (15–20). The rate-limiting step for C–C bond formation between hydrogen-deficient "CH_x" adsorbed fragments appeared to be the methane adsorption, after which hydrocarbons could be displaced from the surface of the metal by competitive adsorption, of CO in particular (21). The hydrogenation step could then be considered as short. However, this could not explain why more hydrocarbons were produced when the coverage in carbon was low in the experiments performed in van Santen's group (13).

This controversy over the role played by each step in C–C bonding has been the object of two letters, one from Hlavathy *et al.* supporting the importance of both steps thanks to experiments carried out under vacuum conditions (22), and the answer by Amariglio *et al.*, who pointed out a major difficulty in the topic, i.e., the sensitivity of the nature and reactivity of the carbonaceous deposit to many parameters, leading to a "continuum of situations" (23). Some of these parameters have actually been identified:

—reaction conditions [methane pressure and flow rate, duration of the adsorption step, temperature] (13, 15, 19, 24–27),

—nature of the metallic or bimetallic system, nature of the support, and effect of promoters (13, 19, 27–34),

—metal particle size (13, 32, 35).

Hydrogenation temperature, hydrogen pressure, and flow rate have also been widely studied (18, 24). However, the hydrogenation step has usually been considered not rate limiting and then was chosen short in most cases (a few minutes). To verify the validity of this hypothesis, we investigated the reactivity toward hydrogenation of a carbonaceous deposit obtained through an isothermal procedure. In that case, good results, in terms of hydrocarbon production per metal unit area, were obtained on silica-supported Pt catalysts, among which is the reference catalyst EUROPt-1 (15, 17), which also have the advantage of being less active in hydrogenolysis than other systems, such as ruthenium as metal (19) and acidic zeolites as support (34). On this catalyst, we have chosen to study the reactivity of a carbonaceous deposit obtained by adsorption of methane at 300°C, which proved to give a wide slate of hydrocarbons on subsequent hydrogenation (15).

METHODS

Two Pt/SiO_2 catalysts have been used: the reference catalyst EUROPt-1 (Pt = 6.3 wt%, dispersion measured by H_2–O_2 titrations = 60%) (36) and a sample obtained by sintering of EUROPt-1 at 600°C for 9 h in H_2 [$P(H_2) = 0.33$ bar, $P(He) = 0.66$ bar; total flow rate = 45 ml min^{-1}], called hereafter sintered sample (dispersion measured by H_2–O_2 titrations = 40%). On the sintered sample, transmission electron microscopy showed large metallic ensembles which seemed to be formed by sintering of about 10 small particles in addition to small particles identical to those of fresh EUROPt-1 sample.

The first step (methane adsorption) consisted of flowing a CH_4/He mixture [$P(CH_4) = 0.33$ bar, $P(He) = 0.66$ bar; total flow rate = 15 ml min^{-1}] through the catalyst (200 mg powder) maintained in a tubular glass reactor at 300°C for 5 min for all experiments. In a few experiments, the catalyst was flushed with pure helium flow (30 ml min^{-1}) after methane adsorption and before hydrogenation (intermediate purge). During the hydrogenation step [$P(H_2) =$ 0.33 bar, $P(He) = 0.66$ bar; total flow rate = 45 ml min^{-1}], hydrocarbons that were heavier than methane were trapped in an activated carbon cartridge (Carbotrap 200, Supelco). Analysis of the C_2–C_8 products trapped in the Carbotrap tube was subsequently performed by gas chromatography (chromatograph: Delsi DI 700, column: Chrompack PLOT

25×0.53 m, coated with alumina deactivated by KCl, detection by FID) after flash desorption in a helium backflush flow, by means of a moving furnace heated at 300°C. The reproducibility of the method was checked through a comparison between the amounts of hydrocarbons collected during t min of hydrogenation, and the sum of the amounts collected during t' min ($t' < t$) and within the interval $[t', t]$ min of hydrogenation.

In addition to this analysis of the products accumulated over time, an instantaneous analysis of the gas mixture (from C_1 to C_8) coming from the reactor was possible with the same apparatus: the Carbotrap tube was isolated by commutation of a valve and the tubes connecting the injection valve and the Carbotrap tube were used as a sample loop.

All gases were supplied by Air Liquide. N45 methane was checked not to contain more than 0.05 ppmv of higher hydrocarbons.

The determination of the total amount of carbonaceous species deposited on the catalyst after methane adsorption and purge was performed on a similar apparatus, the chromatographic analysis device of which had been replaced by a mass spectrometer (Delsi Nermag Anagaz 200). It was connected to the exit of the reactor through a heated capillary tube to sample continuously a small part of the gas effluents, with argon as a diluent gas instead of helium. An additional valve allowed us to perform transient experiments using either pure O_2 (flow rate = 10 ml min^{-1}) or a O_2/Ar mixture [$P(O_2) = 0.09$ bar, $P(Ar) = 0.91$ bar; total flow rate = 5.5 ml min^{-1}], to oxidize the carbonaceous species present on the catalyst surface into carbon dioxide, respectively at 300°C or during a temperature ramp from ambient temperature to 400°C [Temperature-programmed -oxidation (TPO), 20°C min^{-1}]. By integrating the $m/e = 28$ and 44 signals (respectively CO^+ and CO_2^+ ions) after calibration with pure CO_2 pulses, it was possible to estimate the amount of carbonaceous species present on the catalyst surface just after methane adsorption or remaining on the catalyst after hydrogenation steps of different duration. The relative amount of carbonaceous species transformed into hydrocarbons was determined by subtraction of the value obtained after hydrogenation from the initial value determined after methane adsorption.

An identical procedure of regeneration of the catalyst in dilute hydrogen [$P(H_2) = 0.33$ bar, $P(He) = 0.66$ bar; total flow rate = 45 ml min^{-1}] at 400°C for 1 h between two cycles of adsorption/hydrogenation or adsorption/hydrogenation/oxidation was sufficient to prevent a deactivation of the catalyst, the activity of which remained unchanged after 30 cycles. However, the number of cycles after which no desorption of hydrocarbons would be observed was not determined. After treatment in hydrogen, the catalyst was flushed with helium during the cooling to 300°C and at 300°C for 2 min before exposure to methane.

RESULTS

1. *Titration of Carbonaceous Species on the Surface of EUROPt-1 Catalyst before and after Hydrogenation*

The quantitative results obtained by oxidation of the carbonaceous deposit at 300°C after methane adsorption or after hydrogenations of various duration are shown in Fig. 1 for a constant methane adsorption time of 5 min. Note that to eliminate the gaseous methane, the catalyst was always submitted to a 2-min purge with pure argon between methane adsorption and hydrogenation. The initial quantity of carbon resulting from the methane adsorption was evaluated as 3.7 μmol g^{-1} catalyst (i.e., 0.07% of the methane used for adsorption and 2% of a theoretical monolayer on platinum surface). From the shape of the curve, it appeared that most carbonaceous species present on the catalyst surface after methane adsorption were not hydrogenated instantaneously. After 6 min of hydrogenation, one-half of the carbonaceous species had not been hydrogenated yet; after 15 min, 45% remained untouched. A good simulation of the decreasing curve is obtained on assumption of a first-order reaction between gaseous hydrogen and surface carbonaceous species and taking into account that a part of these species cannot react with hydrogen.

2. *Characterization of the Carbonaceous Species by TPO*

TPO experiments performed after the adsorption step at 300°C, purge, and subsequent fast cooling to ambient temperature in argon flow showed that the surface

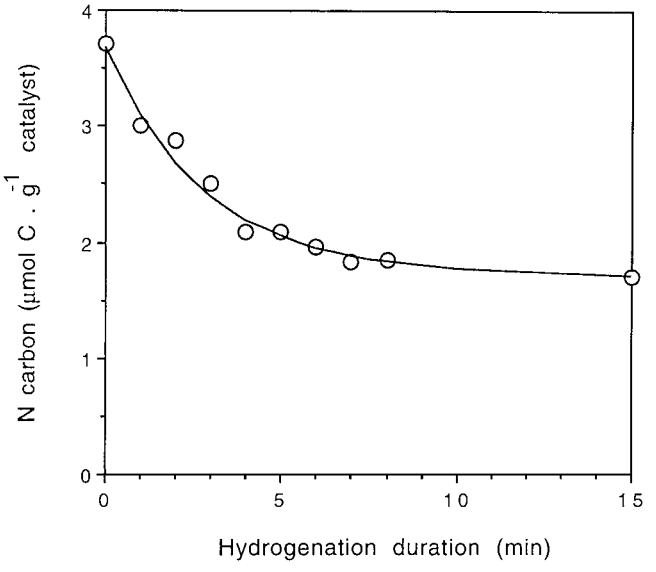

FIG. 1. Titrations by oxygen of amounts of carbonaceous species remaining on EUROPt-1 platinum surface after purge and various hydrogenation durations. ○, Experimental points; —, simulation; temperature of oxidation = 300°C.

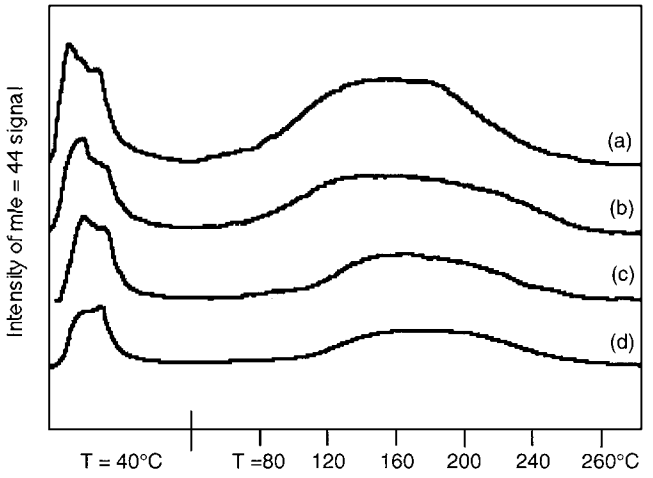

FIG. 2. TPO curves of carbonaceous deposit (intensity of CO_2^+ signal, $m/e = 44$; temperature ramp $= 20°C\ min^{-1}$): (a) after methane adsorption and purge; (b) after 2 min of hydrogenation; (c) after 8 min of hydrogenation; (d) after 15 min of hydrogenation.

carbonaceous species exhibited different reactivities toward oxygen (Fig. 2). A first group of species reacted with oxygen at 40°C [low-temperature peak (LTP)], but at different rates as evidenced by the broad and irregular shape of this oxidation peak. This group represented 25 to 30% of the carbonaceous species present on the surface of the catalyst. A second group of species reacted with oxygen at higher temperatures [broad regular peak between 100 and 250°C, high-temperature peak (HTP)]. The same experiment performed after 2, 8, or 15 min of hydrogenation showed that at any moment of hydrogenation, both groups had been consumed by hydrogen approximately in the same proportions, the first group being attacked mainly through its components most reactive toward oxygen (Table 1).

3. Hydrocarbon Production during the Hydrogenation Step on EUROPt-1 Catalyst (No Intermediate Purge)

The hydrocarbon slate produced during the hydrogenation step was determined at 300°C. The chromatographic analyses performed by use of the sample loop first allowed us to estimate the instantaneous selectivity in C_{2+} hydrocarbons formed by hydrogenation of the carbonaceous deposit compared with the methane produced (Table 2). Approximately one-half of the carbonaceous species gave back methane on hydrogenation, the selectivity in methane decreasing slightly with time. Only alkanes were observed to desorb on hydrogenation.

The quantities of C_{2+} hydrocarbons produced during various hydrogenation durations are presented in Fig. 3a; selectivities calculated on cumulative quantities of hydrocarbons produced during the whole hydrogenation duration appear in Table 3. Ethane, *n*-pentane, and propane appeared to be the main products whatever the hydrogenation duration. The linear alkanes were always produced in larger amounts

TABLE 1

Quantity of Carbon Measured in TPO Experiments Following Hydrogenation[a]

	C surface			C consumed[b]		
t_{H_2} (min)	Total	LTP	HTP	Total	LTP	HTP
0	3.7	0.9	2.8	0	0	0
0–2	2.8	0.7	2.1	0.9	0.2	0.7
0–8	1.9	0.5	1.4	1.8	0.4	1.4
0–15	1.7	0.4	1.3	2.0	0.5	1.5

[a] Expressed in μmol C g^{-1} catalyst. LTP, low-temperature peak; HTP, high-temperature peak.
[b] Obtained by difference.

TABLE 2

Instantaneous Selectivities in Methane and Higher Alkanes during Hydrogenation[a]

t_{H_2} (min)	S_{CH_4} (%)	$S_{C_{2+}}$ (%)
2	54	46
8	49	51
15	43	57

[a] Quantification from data in μmol C g^{-1} catalyst.

TABLE 3

Cumulative Quantities (and Selectivities) of Alkanes Produced during Hydrogenation of the Surface Carbonaceous Species on EUROPt-1[a]

	t_{H_2} (min)				
	0–1.5	0–3	0–8	0–15	0–30
C_2	0.286 (73%)	0.337 (69%)	0.362 (66%)	0.400 (65.5%)	0.462 (63%)
C_3	0.034 (8.5%)	0.051 (10%)	0.059 (11%)	0.070 (11.5%)	0.099 (13.5%)
Iso-C_4	0.004 (1%)	0.006 (1%)	0.007 (1%)	0.010 (2%)	0.017 (2%)
n-C_4	0.012 (3%)	0.018 (4%)	0.021 (4%)	0.025 (4%)	0.040 (5.5%)
Branched C_5	0.007 (2%)	0.014 (3%)	0.015 (3%)	0.020 (3%)	0.025 (3%)
n-C_5	0.040 (10%)	0.053 (11%)	0.055 (10%)	0.056 (9%)	0.058 (8%)
$\sum C_6$	0.007 (2%)	0.008 (1.5%)	0.018 (3%)	0.020 (3%)	0.022 (3%)
$\sum C_{7-8}$	0.001 (0.5%)	0.003 (0.5%)	0.009 (2%)	0.010 (2%)	0.011 (2%)
Total amount of alkanes	0.39	0.49	0.55	0.61	0.73
Total amount of C	1.02	1.33	1.54	1.72	2.08

[a] Values are μmol alkane g^{-1} catalyst (% selectivity).

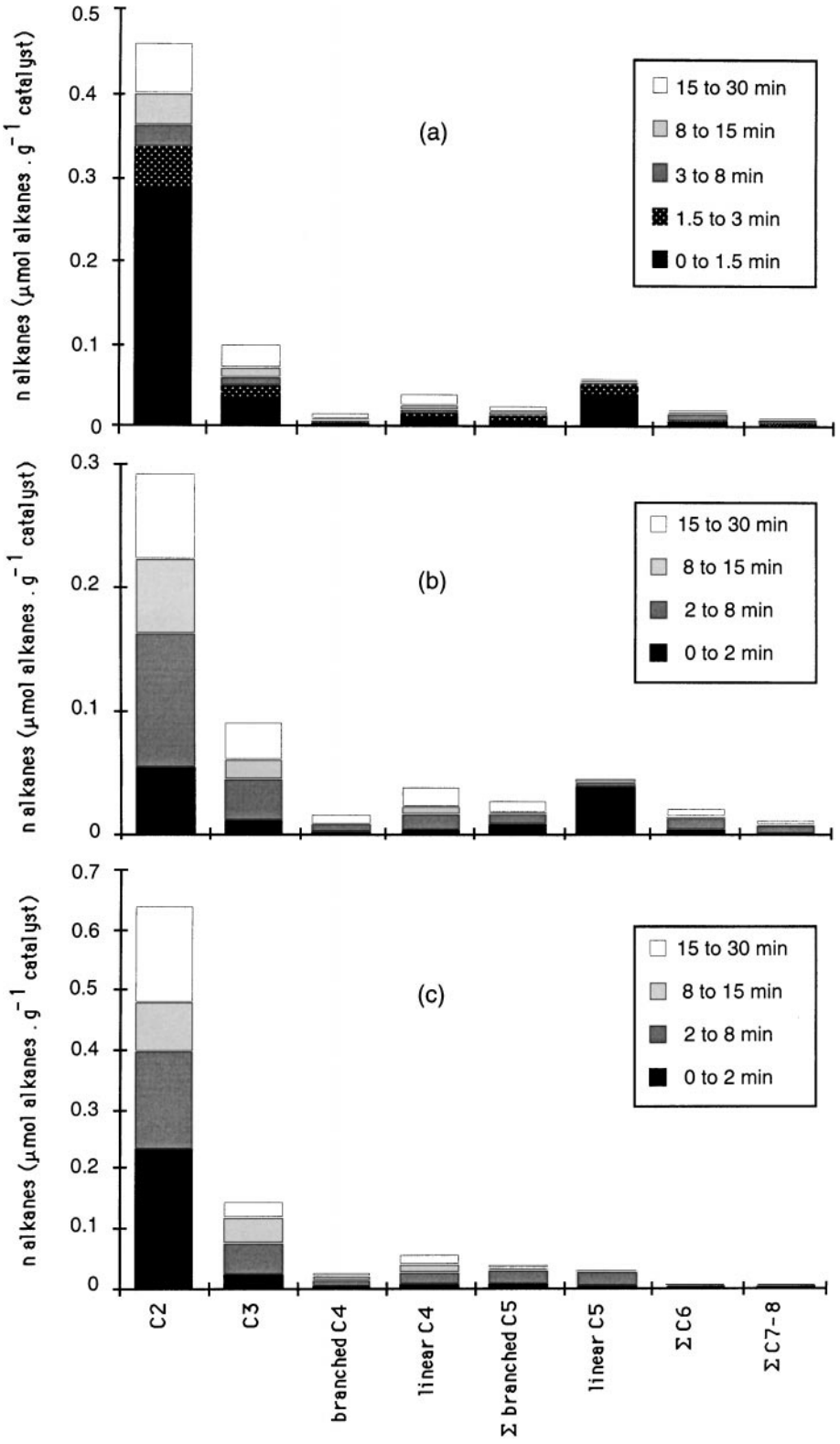

FIG. 3. Hydrocarbon slates as a function of hydrogenation duration on (a) EUROPt-1 without an intermediate purge; (b) EUROPt-1 with an intermediate purge; and a (c) sintered sample.

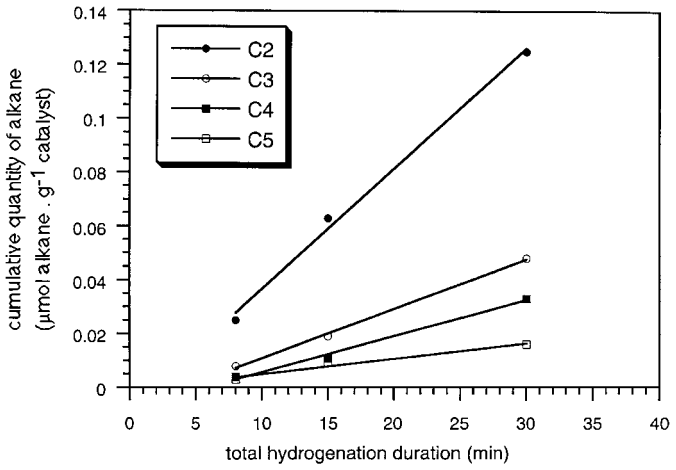

FIG. 4. Cumulative quantities of C_2 to C_5 alkanes produced on EUROPt-1 from 3 min of hydrogenation to t minutes of hydrogenation, as a function of total hydrogenation time t (N[3–t min] = N[0–t min] − N[0–3 min]).

than their branched isomers. In the very first minutes of the hydrogenation, C_2 to C_6 products were mostly detected. A large amount of ethane was produced (more than 60% of the hydrocarbons), as well as a surprisingly large amount of linear pentane, then the second main product after ethane (10%). From 3 min of hydrogenation onward, C_2–C_5 hydrocarbons (linear + branched) appeared to be produced rather constantly with time in hydrogen flow (Fig. 4). The fewer atoms of carbon the alkane contained, the larger the quantity produced; this resulted in a decrease in cumulative selectivity for *n*-pentane during the whole hydrogenation. Heavier hydrocarbons (C_6–C_8) tended to appear mainly after 3 min of hydrogenation and constantly with time. These hydrocarbons were not produced with yields as reproducible as those attached to the production of lighter alkanes.

4. *Effect of a Purge on the Catalytic Properties of EUROPt-1 Catalyst*

The effect of a 2-min purge with pure helium between the two steps was investigated at 300°C. The results are shown in Fig. 3b and Table 4. The purge effect appeared to globally decrease the hydrocarbon production, whatever the duration of the hydrogenation step. Ethane (0.040 μmol g^{-1} catalyst) and, to a lesser extent, *n*-pentane (6×10^{-4} μmol g^{-1} catalyst) desorbed during the purge and could be trapped on activated carbon cartridges. However, this loss had more repercussions on the cumulative quantity of alkanes collected within short hydrogenation times than on the cumulative quantity collected within longer times. The effect was also more important for ethane than for higher alkanes, which were finally produced in amounts similar to those observed in the experiment carried out without an intermediate purge. Compared with this former experiment, the overall hydrocarbon production fell by 45% for 8 min of hydrogenation, 36% for 15 min, and only 27% for 30 min; after 30 min of hydrogenation, ethane production fell by 37%, propane and *n*-butane production by 10% and *n*-pentane production by 25%. If the purge was longer (up to 10 min), it was noted that the production of C_2–C_5 alkanes decreased but the production of heavy hydrocarbons increased.

5. *Hydrocarbon Production during the Hydrogenation Step on the Sintered Sample*

The overall production of hydrocarbons on the sintered sample is shown in Fig. 3c. It was higher than the production of hydrocarbons per gram of EUROPt-1 for equal hydrogenation durations, which means that the sintered sample was more active per unit area of platinum (approximately 1.5 times more active within 30 min of hydrogenation). The main products throughout the hydrogenation period were ethane and propane. The significant difference in selectivities with EUROPt-1 lay in the low production of *n*-pentane, the formation of which appeared to be approximately one-half that observed on EUROPt-1 catalyst under the same conditions (Table 5). In contrast, branched pentanes were produced in larger quantities, which intermediately explains the higher selectivity in pentanes compared

TABLE 4

Cumulative Quantities (and Selectivities) of Alkanes Produced during Hydrogenation of the Surface Carbonaceous Species on EUROPt-1 after Intermediate Purge with Helium[a]

	t_{H_2} (min)			
	0–2	0–8	0–15	0–30
C_2	0.054 (47%)	0.163 (55%)	0.222 (56.5%)	0.292 (55%)
C_3	0.010 (9%)	0.043 (14%)	0.060 (15%)	0.090 (17%)
Iso-C_4	0.001 (1%)	0.006 (2%)	0.008 (2%)	0.015 (3%)
n-C_4	0.003 (3%)	0.015 (5%)	0.022 (5.5%)	0.037 (7%)
Branched C_5	0.006 (5%)	0.014 (5%)	0.018 (4.5%)	0.025 (4.5%)
n-C_5	0.038 (33%)	0.040 (13%)	0.043 (11%)	0.044 (8%)
$\sum C_6$	0.003 (2%)	0.012 (4%)	0.013 (3.5%)	0.020 (3.5%)
$\sum C_{7-8}$	0 (0%)	0.005 (2%)	0.007 (2%)	0.011 (2%)
Total amount of alkanes	0.11	0.30	0.39	0.53
Total amount of C	0.39	0.92	1.18	1.61

[a] Values are μmol alkane g^{-1} catalyst (% selectivity).

TABLE 5

Cumulative Quantities (and Selectivities) of Alkanes Produced during Hydrogenation of the Surface Carbonaceous Species on a Sintered EUROPt-1 Sample[a]

	t_{H_2} (min)			
	0–2	0–8	0–15	0–30
C_2	0.232 (86.5%)	0.394 (70%)	0.480 (66.5%)	0.640 (68%)
C_3	0.021 (8%)	0.075 (13.5%)	0.117 (16%)	0.145 (15.5%)
Iso-C_4	0.002 (1%)	0.012 (2%)	0.020 (2.5%)	0.024 (2.5%)
n-C_4	0.004 (1.5%)	0.023 (4%)	0.039 (5.5%)	0.055 (6%)
Branched C_5	0.006 (2%)	0.030 (5.5%)	0.032 (4.5%)	0.037 (4%)
n-C_5	0.003 (1%)	0.023 (4%)	0.028 (4%)	0.029 (3%)
$\sum C_6$	0 (0%)	0.002 (0.5%)	0.003 (0.5%)	0.004 (0.5%)
$\sum C_{7-8}$	0 (0%)	0.002 (0.5%)	0.003 (0.5%)	0.004 (0.5%)
Total amount of alkanes	0.27	0.56	0.72	0.94
Total amount of C	0.60	1.44	1.89	2.40

[a] Values are μmol alkane g^{-1} catalyst (% selectivity).

with butanes. C_6–C_8 products were produced in very small amounts.

DISCUSSION

Reactivity of the Carbonaceous Species

The reactivity of species resulting from methane adsorption on metallic surfaces has been studied by several authors using various techniques, including temperature-programmed reactions, mainly for methane reforming with CO_2 (37–39). Two types of surface carbonaceous species are usually distinguished by their physicochemical properties and reactivity toward hydrogen or oxygen: "carbidic carbon" stands for the reactive species and "graphitic carbon" for the inert species (13, 40). This widely used nomenclature has been clarified when investigating Fischer–Tropsch synthesis on Ru/SiO_2. ^{13}C NMR has given some insight into the chemical nature of these two groups: carbidic carbon was supposed to be composed of atomic fragments CH_x (C_α) leading to short condensed alkyl chains C_xH_y ($C_{\beta 1}$), while highly condensed forms of hydrocarbon species, heavy alkyl chains ($C_{\beta 2}$), or more certainly sp^2 units (C_γ) could be identified with inert carbon. A purge with inert gas or *in vacuo* could be the cause of a dehydrogenation of the chains, moving the surface equilibria to the formation of graphitic carbon (41).

In agreement with previous experiments using temperature-programmed reactions with hydrogen (15, 20), our results clearly show that the carbonaceous layer obtained by methane adsorption on supported platinum under our conditions (i.e., after a purge with inert gas) contains different species. They do not exhibit a similar reactivity toward oxygen, some species being easily oxidized to carbon dioxide at low temperature with various rates, and others reacting only at higher temperatures. In any case, all the species present on a platinum surface are oxidized at lower temperature than, for instance, the species originating from methane adsorbed on nickel (39), a metal that can form bulk carbides, unlike platinum. Should we brand the most reactive species as "carbidic carbon" and the others as "graphitic carbon"? Although such a classification has been previously used independently of the technique of characterization it originated from (13, 25), we cautiously prefer to specify that it is only for oxidation that the species appear to behave differently. In particular we showed that both types of carbon were attacked by hydrogen during the hydrogenation step and no classification could be made on that basis. It has not been possible to assign the different hydrocarbons produced during hydrogenation to the specific consumption of one of the two groups. Nevertheless, it can be concluded that the hydrogenation of the carbonaceous deposit is not a fast process as it has been assumed or stated before (13, 18, 35), at least for the carbonaceous species obtained in our specific procedure. Hydrocarbons are still produced after 30 min of hydrogenation. Nearly half of the carbon appears to be resistant to hydrogenation. However this inert carbon does not appear to be a poison for the active sites, maybe because of its localization on the support of the metallic active particles (13, 42).

Influence of the Hydrogenation duration on the Hydrocarbon Selectivity

When reacting with hydrogen, half of the carbonaceous species give back methane, while the other half form higher alkanes. If we look at the production of C_{2+} alkanes as a function of the duration of hydrogenation on EUROPt-1, we can discriminate three regimes of production. Mainly ethane and *n*-pentane are produced in the first minutes of hydrogenation. An intermediate purge with helium releases these alkanes in the gas phase and their subsequent production under hydrogenation is lower. It can then be deduced that C–C bonds in these compounds have actually been created during methane adsorption (15). Moreover, the presence of *n*-pentane is characteristic of fresh EUROPt-1 and it may be related to the size or, perhaps more accurately, to the morphology of the platinum particles: it has been shown in the literature that large supported crystallites, like those of our sintered sample, should be more efficient than smaller ones for methane homologation (35), but in our case they are not for *n*-pentane production.

Platinum cuboctahedra featured in EUROPt-1 (36) may favor the initial production of *n*-pentane, which cannot be accomplished by the agglomerated particles of the sintered sample. This initial production of *n*-pentane obviously affects the cumulative quantity of alkanes released during the hydrogenation step, in agreement with previous studies in which an unusual selectivity in *n*-pentane had been noted (15, 34). Besides ethane, C_5 hydrocarbons were also observed to be the most prominent compounds released in the gas phase, after methane and subsequent CO adsorption at 300°C (21). Finally, the same phenomenon was recently underlined on supported rhodium, with a strikingly high selectivity in *n*-pentane over a wide temperature domain (20). It is obvious that this is not in line with what could be expected from the Anderson–Schulz–Flory (ASF) distribution.

Another regime of light C_{2+} alkane production is noted within the course of the hydrogenation. It is characterized by an instantaneous production of C_n alkanes ($2 \leq n \leq 5$) which is constant with time and decreasing with *n* increasing. Two hypotheses can be put forward: either the carbonaceous deposit is undergoing hydrogenolysis, meaning that hydrogen breaks only C–C bonds established during the adsorption step (15); or CH_x fragments, present as such on the surface or resulting from the hydrogenolysis of a heavier carbonaceous compound, are progressively condensed and homologated by hydrogen (13). In hydrogen atmosphere, EUROPt-1 is known to favor the isomerization of alkanes rather than their hydrogenolysis (36). Moreover, hydrogenolysis of a C_3–C_6 mixture on EUROPt-1 showed that pentanes were not consumed below 280°C, giving methane, butane, and propane from terminal hydrogenolysis (15). As propane and butanes were not hydrogenolyzed below 320°C, an excess of C_3 and C_4 compounds at 300°C resulted, which is not the case in our experiments. In contrast, a condensation of the fragments during hydrogenation could occur regularly and statistically. A plot of the logarithm of cumulative collected quantities of C_2–C_5 alkanes (C_n including the branched alkanes with *n* carbon atoms) as a function of *n* after subtraction of the alkanes produced in the first 3 min of hydrogenation (Fig. 5A) now shows better agreement with the ASF model (5, 13). A similar graph can be obtained for the experiment carried out on EUROPt-1 with an intermediate purge, after subtraction of the alkanes produced in the first 2 min of hydrogenation (Fig. 5B). In that case, the slope of the straight lines is higher than in the experiment carried out without purge, which could show a higher probability of coupling between surface species transformed during the 2-min purge. This model could probably fit better our observations by taking into account the specific probability of formation of branched alkanes through condensation of a CH_x unit on a secondary carbon of the growing chain, or the nondegradative isomerization properties of EUROPt-1 (36). However, it cannot apply

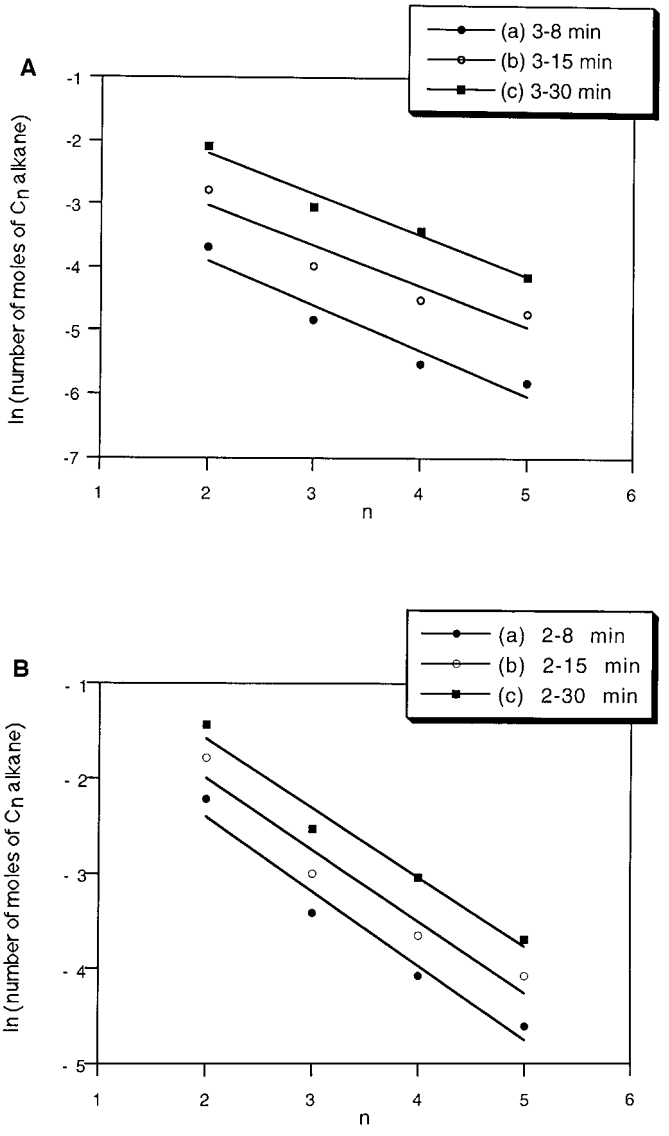

FIG. 5. (A) Anderson–Schulz–Flory plot of the cumulative quantities of C_2–C_5 hydrocarbons produced on EUROPt-1 between (a) 3 and 8 min of hydrogenation; (b) 3 and 15 min of hydrogenation; (c) 3 and 30 min of hydrogenation (no intermediate purge). (B) Anderson–Schulz–Flory plot of the cumulative quantities of C_2–C_5 hydrocarbons produced on EUROPt-1 between (a) 2 and 8 min of hydrogenation; (b) 2 and 15 min of hydrogenation; (c) 2 and 30 min of hydrogenation (with intermediate purge).

satisfactorily to the production of hydrocarbons on the sintered sample, whose production in pentanes is most of the time higher than the production in butanes.

Finally, the heavier alkanes ($>C_6$) are produced after long durations of hydrogenation and cannot be placed in the same category as the hydrocarbons described above. As their production seems to be enhanced if a purge with helium is carried out before the hydrogenation step, it can be supposed that they are produced by the slow hydrogenolysis of dehydrogenated and condensed carbonaceous species similar to graphitic carbon (23).

It must be noted that in two recent articles from Nancy, in which the reactivities of silica-supported ruthenium and platinum (EUROPt-1) toward the nonoxidative conversion of methane to higher hydrocarbons were compared (43, 44), the results obtained by varying the adsorption and hydrogenation step temperatures led the authors to assume the existence of several types of carbonaceous species present on the catalyst surface. They would differ by their molecular weight, their stabilization by specific sites of the catalyst, and consequently their reactivity toward hydrogen. They would lead to different hydrocarbons on hydrogenation, produced by hydrogenolysis or Fischer–Tropsch-like coupling. A kinetic study of the hydrogenation step was mentioned to be reported in a next article. Additionally, a recent contribution from Guczi *et al.* showed that at least on Pd–Co/SiO_2 catalysts, the combination of methane chemisorption and hydrogenation in the same step could be more efficient for heavy hydrocarbon production than the classic two-step sequence (45).

Model

We can propose a model for the mechanism of formation of alkanes during the nonoxidative homologation of methane that could take into account our observations on EUROPt-1 for a methane adsorption step performed at 300°C and a hydrogenation step performed at the same temperature. The classification developed by Carstens and Bell for the surface carbonaceous species on ruthenium is used by analogy (25).

During the first step, methane decomposes on the metallic surface into CH_x fragments while H_2 evolves from the catalyst and is carried away by the gas flow:

$$CH_4 \rightarrow CH_{x\,\mathrm{ads}} + (4-x)/2H_{2\,\mathrm{g}}.$$

Unlike in Fischer–Tropsch synthesis, in which the prior dissociation of CO is required, the adsorbed CH_x fragments can immediately condense into heavier species, first into C_2 units (C_α), thought to be the initiating unit in Fischer–Tropsch synthesis and in CH_x coupling on monocrystals (46, 47), then into longer chains formed by the homologation of C_1 and C_2 bricks (C_β). The heaviest and most inert species ($C_{\beta 2}$) stay at the metal–support interface, where they will not be able to poison the surface for the subsequent hydrogenation process, and lighter species ($C_{\beta 1}$) grow on specific active sites, which we will try to characterize further, leading at the utmost in our case to a five-carbon precursor on fresh EUROPt-1:

$$2CH_{x\,\mathrm{ads}} \rightarrow C_2H_{y\,\mathrm{ads}} \xrightarrow{n\,CH_{x\,\mathrm{ads}}} \begin{cases} C_2, C_5\ \text{precursors}_{\mathrm{ads}}\ (C_{\beta 1}) \\ \text{long chains}_{\mathrm{ads}}\ (C_{\beta 2}) \end{cases}$$

At this moment, the species most reactive toward hydrogenation would be mainly C_1, C_2, and C_5 species. The formation of such reactive carbonaceous species rather than inert ones would be favored at low coverages (13) and mild temperatures (20). An intermediate purge in helium would cause the release of some ethane and traces of *n*-pentane in the gas phase, without depleting much the C_5 precursor reservoir, as well as a global dehydrogenation of the surface species, toward the formation of heavier hydrocarbon precursors:

$$C_2, C_5\ \text{precursors}_{\mathrm{ads}}\ (C_{\beta 1}) \xrightarrow{\mathrm{He}} C_5\ \text{precursors}_{\mathrm{ads}} + C_2H_{6\,\mathrm{g}}$$

$$\text{long chains}_{\mathrm{ads}}\ (C_{\beta 2}) \xrightarrow{\mathrm{He}} \text{heavy hydrocarbons}_{\mathrm{ads}} + H_{2\,\mathrm{g}}$$

During the first minutes of the hydrogenation, the light chains that have been built during the adsorption step and could be possibly displaced by CO adsorption as unsaturated hydrocarbons (21) give mostly ethane and *n*-pentane on fresh EUROPt-1:

$$C_2, C_5\ \text{precursors}_{\mathrm{ads}} + H_{2\,\mathrm{g}} \rightarrow C_2H_{6\,\mathrm{g}} + C_5H_{12\,\mathrm{g}}.$$

Several processes can then basically occur on the metallic surface:

(i) formation of methane from hydrogenation of C_α fragments and possibly terminal hydrogenolysis of longer chains,

(ii) dynamic homologation of small fragments originating from C_α and $C_{\beta 1}$, migrating onto the active sites, with creation of new C–C bonds in a statistical manner (this leads to C_2–C_5 hydrocarbons with an ASF distribution),

(iii) decomposition of heavy species to new C_α and $C_{\beta 1}$ fragments that can condense under the action of hydrogen as in (ii),

(iv) slow hydrogenolysis of the heavier fractions ($C_{\beta 2}$), into long chains (this leads to irregular C_6–C_8 production, depending on the history of the catalyst and the subsequent behavior of its "graphitic" reservoir).

$$\begin{array}{ccccc} \text{long chains}_{\mathrm{ads}}\ (C_{\beta 2}) & \xrightarrow{H_{2\,\mathrm{g}}} & n\,CH_{x\,\mathrm{ads}} & \xrightarrow{H_{2\,\mathrm{g}}} & C_2\text{–}C_5\ \text{hydrocarbons}_{\mathrm{g}} \\ {\scriptstyle H_{2\,\mathrm{g}}}\downarrow & & {\scriptstyle H_{2\,\mathrm{g}}}\downarrow & & \\ C_6\text{–}C_8\ \text{hydrocarbons}_{\mathrm{g}} & & CH_{4\,\mathrm{g}} & & \end{array}$$

Initial Selectivity in n-Pentane: An Organometallic Analogy

The typical feature of methane oligomerization on EUROPt-1, as well as on other metallic catalysts as reported above, is a dramatic initial production of *n*-pentane, which we assume is the longest chain stable on specific active sites during the adsorption step. This remarkable feature may give us some hints to the nature of these active sites. The faces of EUROPt-1 platinum cuboctahedra can be proposed as potential active sites, since they are known to stabilize C_5 hydrocarbons, which accounts for the high

activity of EUROPt-1 in skeletal isomer formation for hexane (36). Isomerization reactions on crystalline faces could also explain the high selectivity in branched pentanes on the sintered sample. However, it could not explain why the sintered sample with its larger crystalline faces cannot initially produce hydrocarbons higher than pentane (unless the condensed species are too heavy to be hydrogenated). The marked difference existing between the fresh and sintered catalysts allows us to suppose that these specific active sites are rather the coordinately unsaturated atoms of the platinum particles, i.e., the edges and corners, scarcer on the sintered sample and shown to be active toward methane activation on platinum clusters (48). On ruthenium monocrystals, Wu and Goodman have already shown that corrugated and noncorrugated faces can stabilize different carbonaceous species resulting from CH_x coupling (49). Is our hypothesis compatible with the chemistry of platinum and hydrocarbons?

It can be noted first that platinum atoms in low coordination on EUROPt-1 catalyst are not thought to increase the C–C splitting probability during reactions between hydrocarbons and hydrogen (50). We can now consider the mechanism leading to C_5 precursors from an organometallic point of view, as a CH_x coupling and insertion process occurring on an hydrocarbon chain supported by atoms in low coordination from corrugated metallic surfaces (51). In this hypothesis, alkyl platinum complexes L_2PtR_2 ($L =$ phosphine, $R =$ alkyl group) and platinacycles $L_2Pt(1,n\text{-}(CH_2)_n)$, the chemistry of which is well documented (52–55), can be taken as model compounds. The alkyl chains are reactive toward hydrogen and they lead to alkanes when hydrogenated in solution in the presence of platinum black (56). They can also be homologated by insertion of a CH_2 group coming, for example, from the solvent CH_2Cl_2 (57) or a neighboring CH_3 group (58). The relative stability of the acyclic alkyl compounds and of their platinacycle counterparts was studied in solution and by thermal analysis experiments (53, 58, 60–62). When the acyclic alkyl groups have a hydrogen atom in β-position, the complexes decompose by β-elimination of the hydrogen onto the platinum atom and release of an alkene molecule (53, 55, 58, 61). Otherwise C–C bond splittings, formation of large metallacycles, or reductive eliminations of linear or cyclic hydrocarbons are observed (56, 58, 62–65). In contrast, platinacycles are found to be more stable than complexes with acyclic ligands, with slower rates of decomposition at a given temperature (53). Their strain energy is lower than in corresponding hydrocarbon cycles (66) and for the shortest rings, no hydrogen is close enough to the platinum atom to permit a β-elimination process; the main decomposition process in solution occurs by intermolecular transfer of hydride species (67). The largest cycle stable toward β-elimination is the six-membered ring of a platinacyclohexane, i.e., a cycle formed by one platinum atom and a five-carbon hydrocarbon chain (53).

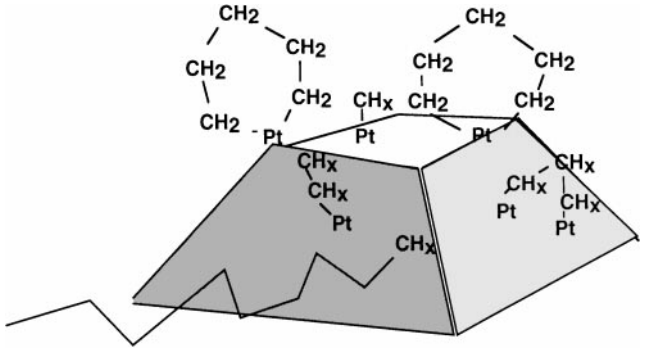

FIG. 6. Model of the carbonaceous species supported on a EUROPt-1 platinum crystallite after methane adsorption.

If the same criteria of stability applied to the carbonaceous species on platinum atoms in low-coordinate position, it could mean that the most stable species supported by these atoms should be cyclic, grown from metallacyclic C_3 units—since it would be unlikely that the terminal methyl of a *n*-pentyl linear chain could be activated by the platinum atoms to give eventually a cycle—and could not have more than five atoms of carbon (Fig. 6). Such supported cyclic species have already been postulated on corrugated surfaces, to explain the mechanisms of ring opening, hydrogenolysis, or hydrogenation of hydrocarbons using organometallic analogies (68–70). This hypothesis may be checked by using D_2 as hydrogenating reactant in the second step of the oligomerization process and comparing the positions of deuteration in pentanes produced before and after 3 min of hydrogenation. In the first case, deuteration should occur only at the extremities of the carbonaceous chain.

CONCLUSIONS

The two-step nonoxidative oligomerization of methane on Pt/SiO_2 catalyst (EUROPt-1) at 300°C is based on the concomitant hydrogenation of various carbonaceous species obtained by methane adsorption under flow conditions and which can be distinguished by their reactivity toward oxygen. Methane is the main product of hydrogenation but one-half of the reactive carbonaceous species deposited on the catalyst surface form other alkanes. Three modes of production of alkanes can be distinguished during the hydrogenation step, leading to distinct slates in hydrocarbons. First, ethane and *n*-pentane are the main products released from fresh EUROPt-1 in the first minutes of reaction. The creation of C–C bonds between carbonaceous species as early as the methane adsorption step probably leads on EUROPt-1 to specific precursors of *n*-pentane. An organometallic analogy with the stability of platinacyclic complexes allows us to suppose that these precursors are cyclic and supported by coordinately unsaturated atoms of platinum, at the edges and corners of the metallic

particles. Second, new C–C bonds can be created within the course of the hydrogenation step through a statistical and dynamic homologation mechanism, giving a slate in C_2–C_5 alkanes in line with the Anderson–Schulz–Flory model. Finally, higher hydrocarbons are slowly produced by hydrogenolysis of heavy carbonaceous compounds, maybe located at the interface between platinum and silica.

ACKNOWLEDGMENT

The authors thank Dr. Ralf Wyrwa (Institut für Anorganische und Analytische Chemie, Friedrich Schiller Universität Jena, Germany) for providing information concerning the thermal decomposition of molecular platinacycles.

REFERENCES

1. Rojey, A., and Jaffret, C., "Natural Gas—Production, Processing, Transport." Institut Français du Pétrole Publications, Editions Technip, Paris, 1997.
2. Fox, J. M., III, *Catal. Rev.-Sci. Eng.* **35**, 169 (1993).
3. Maxwell, I. E., Naber, J. E., and de Jong, K. P., *Appl. Catal. A* **113**, 153 (1994).
4. Rostrup-Nielsen, J. R., *Catal. Today* **21**, 257 (1994).
5. Iglesia, E., Reyes, S. C., Madon, R. J., and Soled, S. L., *Adv. Catal.* **39**, 221 (1993).
6. Chang, C. D., *Stud. Surf. Sci. Catal.* **61**, 393 (1991).
7. Fujimoto, K., *Stud. Surf. Sci. Catal.* **81**, 73 (1994).
8. Guczi, L., van Santen, R. A., and Sarma, K. V., *Catal. Rev.-Sci. Eng.* **38**, 249 (1996).
9. Amariglio, H., Saint-Just, J., and Amariglio, A., *Fuel Process. Technol.* **42**, 291 (1995). See also Amariglio, H., and Saint-Just, J., French Patent Application 9,009,340 (July 20th, 1990); Koerts, T., and van Santen, R. A., U.K. Patent Application 2,253,858A (March 21, 1991); Amariglio, H., and Saint-Just, J., U.S. Patent 5,414,176 (May 9, 1995).
10. Koerts, T., Leclercq, P. A., and van Santen, R. A., *J. Am. Chem. Soc.* **114**, 7272 (1992).
11. Lefort, L., Amariglio, A., and Amariglio, H., *Catal. Lett.* **29**, 125 (1994).
12. Koerts, T., and van Santen, R. A., *J. Chem. Soc. Chem. Commun.*, 1281 (1991).
13. Koerts, T., Deelen, M. J. A., and van Santen, R. A., *J. Catal.* **138**, 101 (1992).
14. Koerts, T., and van Santen, R. A., *J. Mol. Catal.* **74**, 185 (1992).
15. Belgued, M., Amariglio, A., Paréja, P., and Amariglio, H., *J. Catal.* **159**, 441, 449 (1996).
16. Belgued, M., Amariglio, H., Paréja, P., and Amariglio, A., *Nature* **352**, 789 (1991).
17. Belgued, M., Amariglio, H., Paréja, P., Amariglio, A., and Saint-Just, J., *Catal. Today* **13**, 437 (1992).
18. Amariglio, H., Paréja, P., and Amariglio, A., *Catal. Today* **25**, 113 (1995).
19. Belgued, M., Amariglio, A., Lefort, L., Paréja, P., and Amariglio, H., *J. Catal.* **161**, 282 (1996).
20. Paréja, P., Molina, S., Amariglio, A., and Amariglio, H., *Appl. Catal. A* **168**, 289 (1998).
21. Amariglio, H., Belgued, M., Paréja, P., and Amariglio, A., *Catal. Lett.* **31**, 19 (1995).
22. Hlavathy, Z., Paál, Z., and Tetényi, P., *J. Catal.* **166**, 118 (1997).
23. Amariglio, A., Paréja, P., and Amariglio, H., *J. Catal.* **166**, 121 (1997).
24. Koranne, M. M., Goodman, D. W., and Zajac, G. W., *Catal. Lett.* **30**, 219 (1995).
25. Carstens, J. N., and Bell, A. T., *J. Catal.* **161**, 423 (1996).
26. Monteverdi, S., Amariglio, A., Paréja, P., and Amariglio, H., *J. Catal.* **172**, 259 (1997).
27. Solymosi, F., Erdöhelyi, A., and Cserényi, J., *Catal. Lett.* **16**, 399 (1992).
28. Solymosi, F., Erdöhelyi, A., Cserényi, J., and Felvégi, A., *J. Catal.* **147**, 272 (1994).
29. Solymosi, F., and Cserényi, J., *Catal. Today* **21**, 561 (1994).
30. Solymosi, F., and Cserényi, J., *Catal. Lett.* **34**, 343 (1995).
31. Guczi, L., Sarma, K. V., and Borkó, L., *Catal. Lett.* **39**, 43 (1996).
32. Boskovic, G., Zadeh, J. S. M., and Smith, K. J., *Catal. Lett.* **39**, 163 (1996).
33. Guczi, L., Sarma, K. V., and Borkó, L., *J. Catal.* **167**, 495 (1997).
34. Mielczarski, E., Monteverdi, S., Amariglio, A., and Amariglio, H., *Appl. Catal. A* **104**, 215 (1993).
35. Cheikhi, N., Ziyad, M., Coudurier, G., and Védrine, J. C., *Appl. Catal. A* **118**, 187 (1994).
36. Bond, G. C., and Paál, Z., *Appl. Catal. A* **86**, 1 (1992).
37. Solymosi, F., Kutsán, G., and Erdöhelyi, A., *Catal. Lett.* **11**, 149 (1991).
38. Tsipouriari, V. A., Efstathiou, A. M., and Verykios, X. E., *J. Catal.* **161**, 31 (1996).
39. Kroll, V. C. H., Swaan, H. M., Lacombe, S., and Mirodatos, C., *J. Catal.* **164**, 387 (1997).
40. Bell, A. T., *Stud. Surf. Sci. Catal.* **48**, 91 (1989).
41. Duncan, T. M., Winslow, P., and Bell, A. T., *J. Catal.* **93**, 1 (1985).
42. Yokomizo, G. H., and Bell, A. T., *J. Catal.* **119**, 467 (1989).
43. Amariglio, A., Belgued, M., Paréja, P., and Amariglio, H., *J. Catal.* **177**, 113 (1998).
44. Amariglio, H., Belgued, M., Paréja, P., and Amariglio, A., *J. Catal.* **177**, 121 (1998).
45. Guczi, L., Borkó, L., Koppány, Zs., and Mikuzami, F., *Catal. Lett.* **54**, 33 (1998).
46. Wu, M. C., Lenz-Solomon, P., and Goodman, D. W., *J. Vac. Sci. Technol. A* **12**, 2205 (1994).
47. Long, H. C., Turner, M. L., Fornasiero, P., Kaspar, J., Graziani, M., and Maitlis, P. M., *J. Catal.* **167**, 172 (1997).
48. Trevor, D. J., Cox, D. M., and Kaldor, A., *J. Am. Chem. Soc.* **112**, 3742 (1990).
49. Wu, M. C., and Goodman, D. W., *J. Am. Chem. Soc.* **116**, 1364 (1994).
50. Bond, G. C., and Lin, X., *J. Catal.* **168**, 207 (1997).
51. Leconte, M., *J. Mol. Catal.* **86**, 205 (1994).
52. Biefeld, C. G., Eick, H. A., and Grubbs, R. H., *Inorg. Chem.* **12**, 2166 (1973).
53. McDermott, J. X., White, J. F., and Whitesides, G. M., *J. Am. Chem. Soc.* **95**, 4551 (1973).
54. De Boer, H. J. R., Akkerman, O. S., and Bickelhaupt, F., *J. Organomet. Chem.* **336**, 447 (1987).
55. Fröhlich, H. O., Wyrwa, R., and Görls, H., *Angew. Chem. Int. Ed. Engl.* **32**, 387 (1993).
56. Miller, T. M., Izumi, A. I., Shih, Y. S., and Whitesides, G. M., *J. Am. Chem. Soc.* **110**, 3146 (1988); Miller, T. M., McCarthy, T. J., and Whitesides, G. M., *J. Am. Chem. Soc.* **110**, 3156 (1988); Miller, T. M., and Whitesides, G. M., *J. Am. Chem. Soc.* **110**, 3164 (1988).
57. Young, G. B., and Whitesides, G. M., *J. Am. Chem. Soc.* **100**, 5808 (1978).
58. Brown, M. P., Hollings, A., Houston, K. J., Puddephatt, R. J., and Rashidi, M., *J. Chem. Soc. Dalton Trans.*, 786 (1976).
59. Cheetham, A. K., Puddephatt, R. J., Zalkin, A., Templeton, D. H., and Templeton, L. K., *Inorg. Chem.* **15**, 2997 (1976).
60. McDermott, J. X., White, J. F., and Whitesides, G. M., *J. Am. Chem. Soc.* **98**, 6521 (1976).
61. Fröhlich, H. O., Wyrwa, R., Görls, H., and Pieper, U., *J. Organomet. Chem.* **471**, 23 (1994).

62. Wyrwa, R., Fröhlich, H. O., and Görls, H., *J. Organomet. Chem.* **503**, 135 (1995).
63. Wyrwa, R., Fröhlich, H. O., and Görls, H., *J. Organomet. Chem.* **491**, 41 (1995).
64. Foley, P., DiCosimo, R., and Whitesides, G. M., *J. Am. Chem. Soc.* **102**, 6713 (1980).
65. Whitesides, G. M., Hackett, M., Brainard, R. L., Lavalleye, J. P. P. M., Sowinski, A. F., Izumi, A. N., Moore, S. S., Brown, D. W., and Staudt, E. M., *Organometallics* **4**, 1819 (1985).
66. DiCosimo, R., Moore, S. S., Sowinski, A. F., and Whitesides, G. M., *J. Am. Chem. Soc.* **104**, 124 (1982).
67. Miller, T. M., and Whitesides, G. M., *Organometallics* **5**, 1473 (1986).
68. Engstrom, J. R., Goodman, D. W., and Weinberg, W. H., *J. Am. Chem. Soc.* **108**, 4653 (1986).
69. Engstrom, J. R., Goodman, D. W., and Weinberg, W. H., *J. Phys. Chem.* **94**, 396 (1990).
70. Martel, R., Rochefort, A., and McBreen, P. H., *J. Am. Chem. Soc.* **120**, 2421 (1998).